Synthesis, Structural Characterization, and Physical Properties of Lamellar MPS_3 Crystals Intercalated with Tetrathiafulvalene (M = Mn, Fe)

Anne Léaustic, Jean Paul Audière, Pascal G. Lacroix, and René Clément*

Laboratoire de Chimie Inorganique, CNRS U.R.A. 420, Université Paris Sud, 91405 Orsay Cedex, France

Léticia Lomas

Universidad Autonoma Metropolitana Iztapalapa, Departamento Quimica, P.O. Box 55-534, 09340 Mexico D.F.

Alain Michalowicz

Laboratoire de physique des milieux desordonnés, Université Paris Val de Marne (Créteil) et L.U.R.E., Université Paris Sud, 91405 Orsay Cedex, France

William R. Dunham and Anthony H. Francis

Departement of Chemistry, The University of Michigan, Ann Arbor, Michigan 48109

Received July 26, 1994. Revised Manuscript Received March 10, 1995[⊗]

This paper gives a detailed account on the synthesis, physical properties and spectroscopic characterization of the MPS_3–tetrathiafulvalene intercalates $M_{1-x}PS_3(TTF)_{\sim 2x}$ (M = Mn, Fe). These materials have been obtained by applying ion-exchange procedures to MPS_3 alkylammonium preintercalates. Magnetic and electrical measurements have been carried out on powdered and quasimonocristalline samples of the intercalates. While $Mn_{1-x}PS_3(TTF)_{\sim 2x}$ exhibits a thermally activated conductivity, the analogue $Fe_{1-x}PS_3(TTF)_{\sim 2x}$ possesses a metallic character. The magnetic properties arise from localized spins of the M^{2+} cations interacting antiferromagnetically. EXAFS data at the metal K edge show that TTF^+ insertion results in an increase of the M–M bond length by ≈0.1 Å and an increase of disorder. ^{57}Fe Mössbauer data on $Fe_{1-x}PS_3(TTF)_{\sim 2x}$ reveal the occurrence of ferric ions (14%) in the host lattice. This result provides an interpretation for the metallic character of this intercalate in terms of partial electron tranfer between the Fe^{2+} ions of the $FePS_3$ lattice and the TTF^+ species, leading to $TTF^+/TTF°$ mixed valent stacking. ^{57}Fe Mössbauer data on $Fe_{1-x}PS_3(TTF)_{\sim 2x}$ reveal the occurrence of ferric ions (14%) in the host lattice. The Raman spectrum of this intercalate shows the presence of neutral TTF°, of TTF^+ cations, and of mixed-valent TTF species. The origin of the metallic character of the $Fe_{1-x}PS_3(TTF)_{\sim 2x}$ intercalate is discussed in terms of partial electron transfer between the Fe^{2+} ions of the $FePS_3$ lattice and the TTF^+ species initially introduced by ion exchange.

Introduction

The MPS_3 compounds, where M stands for a metal in the +2 oxidation state, form a class of lamellar semiconductors[1–4] with the $CdCl_2$ structural type (Figure 1). These materials occupy a unique position among the chalcogenide-based layered materials, as they exhibit two very different types of intercalation chemistry (for a review, see refs 5–7):

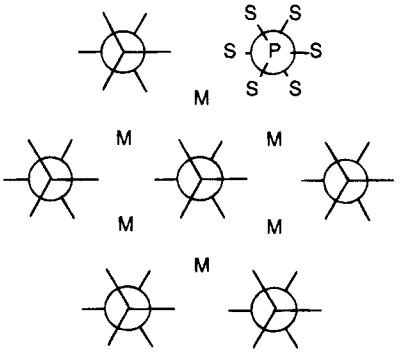

Figure 1. Schematic top view of a MPS_3 slab, array of M^{2+} cations coordinated to $P_2S_6^{4-}$ bridging ligands.

A first type based on Redox processes: the materials react with electron donating species such as lithium, butyllithium, cobaltocene, and some of them (M = Fe, Ni) have been shown to act as efficient cathodes in reversible lithium batteries.[8–12]

[⊗] Abstract published in *Advance ACS Abstracts,* May 1, 1995.

(1) Klingen, W.; Ott, R.; Hahn, H. *Z. Anorg. Allg. Chem.* **1973**, *396*, 271.
(2) Klingen, W.; Eulenberger, G.; Hahn, H. *Z. Anorg. Allg. Chem.* **1973**, *401*, 97.
(3) Prouzet, E.; Ouvrard, G.; Brec, R. *Mater. Res. Bull.* **1986**, *21*, 195.
(4) Ouvrard, G.; Brec, R.; Rouxel, J. *Mater. Res. Bull.* **1985**, *20*, 1181.
(5) Brec, R. *Solid State Ionics* **1986**, *22*, 3 and references therein.
(6) O'Hare, D. In *Inorganic Materials*; Bruce D., O'Hare, D., Eds.; John Wiley: New York; 1992; p 165.
(7) Jacobson, A. In *Solid State Chemistry Compounds*; Cheetham, A. K., Day, P., Eds.; Oxford Science Publications: Clarendon Press, Oxford, 1992; p 204.

0897-4756/95/2807-1103$09.00/0

A second type based on a unique cation-exchange process,[13-17] in which the electrical charge of the cationic guest species entering the host lattice is counterbalanced by the loss of intralayer M^{2+} ions. An important feature of the ion exchange chemistry is that it yields intercalates generally air stable, well crystallized and, for some of them, optically transparent or pale colored.[18-21] These nanocomposites are often interesting materials that display original properties with respect to the parent compounds: for instance, ferrimagnetic intercalates with high Curie temperatures have been obtained on intercalating $MnPS_3$ and $FePS_3$,[17,22-25] Second harmonic generation has been recently obtained from $CdPS_3$ intercalated by asymmetric stilbazolium chromophores.[26]

The reaction of tetrathiafulvalene and derivatives with layered materials has been studied in a number of cases, and it is envisaged as a new approach to the synthesis of low dimensional organic–inorganic metals. A layered material may act as a macroionic host capable of enforcing segregation and able to accept electrons from (or donate to) suitable guest species, thereby causing mixed valency. For instance, guest-to-host electron donation has been evidenced upon insertion of tetrathiafulvalene (TTF) and various derivatives into FeOCl, silicates, and V_2O_5.[27-32] Recently, Averill et al. obtained a semiconducting intercalate with high conductivity and low activation energy upon inserting BEDT–TTF into FeOCl.[33,34]

Our approach is quite different. The MPS_3 host lattice has no oxidizing character, in contrast to FeOCl or V_2O_5. Our stategy therefore consists in inserting TTF^+ cationic species by ion exchange, expecting that a redox process between two internal Redox couples will occur and cause mixed valency. We have reported previously that TTF^+ cations could actually be inserted into MPS_3 (M = Mn, Cd)[35] and that insertion of TTF^+ cations into $FePS_3$ led to an intercalate which exhibited electrical properties drastically modified with respect to those of the pristine host material (appearance of a metallic character).[36] However, the materials were poorly characterized. A study of the IR and UV visible spectra of the $MnPS_3$–TTF intercalate recently appeared,[37] which confirmed our suggestions of mixed valency.[35,36] The present article describes detailed new results on the synthesis, physical properties, and spectroscopic characterization of the TTF intercalates of $MnPS_3$ and $FePS_3$, which allow a reasonable understanding of their properties.

Experimental Section

The materials were characterized by X-ray powder diffraction using a Siemens diffractometer and a Seeman Bohlin camera. Infrared spectra were obtained as KBr pellets using a Perkin-Elmer 883 spectrometer. Elemental analyses were obtained from the CNRS analytical service.

The dc electrical conductivity of the intercalates along the plane of the layers were measured using a classical four probe technique. Large (5 × 5 × 0.05 mm) quasimonocrystalline platelets of the intercalates were prepared following the above-described procedure, increasing reaction duration by a factor of about 3. Gold electrodes were deposited on the platelets by evaporation under vacuum, and the latter were then glued on thin glass plates fixed on a copper block fitted with a thermocouple and cooled with a flow of nitrogen or heated by electrical means. Measurements were carried out under primary vacuum.

The temperature dependence of the magnetic susceptibility of the powdered samples (about 5 mg) has been studied with a Faraday magnetometer fitted with an Oxford Instruments cryostat operating between 4.2 K and room temperature.

EXAFS measurements were carried out on the DCI storage ring at LURE, the French center for synchrotron radiation. The monochromator was a Si(311) channel cut crystal on the EXAFS III port. The EXAFS spectra of pure $FePS_3$, $Fe_{0.85}PS_3(Et_4N^+)_{0.3}$, and $Fe_{0.82}PS_3(TTF)_{0.38}$ have been recorded at room temperature between 7000 and 8000 eV (Fe K edge = 7112 eV). The data have been analyzed and fitted according to standard procedures already described with the EXAFS analysis programs.[38-43]

Mössbauer spectra, taken from 77 to 300 K were recorded and processed using previously published procedures devel-

(8) Brec, R.; Schleich, D.; Ouvrard, G.; Loiuisy,A.; Rouxel, J. *Inorg. Chem.* **1979**, *18*, 1814.
(9) Clément, R.; Green, M. L. H. *J. Chem. Soc., Dalton Trans.* **1979**, 1566.
(10) Berthier, J; Chabre, Y; Minier, M. *Solid State Commun.* **1978**, *28*, 327.
(11) J. Rouxel, J.; Brec, R. *Annu. Rev. Mater. Sci.* **1986**, *16*, 137.
(12) Fatseas, G. A.; Evain, M.; Ouvrard, G.; Brec, R.; WhangBo, M. H. *Phys. Rev. B* **1987**, *35*, 3082.
(13) Clément, R. *J. Chem. Soc., Chem. Commun.* **1980**, 647.
(14) Clément, R. *J. Am. Chem. Soc.* **1981**, *103*, 6998.
(15) Clément, R.; Garnier, O.; Jegoudez, J. *Inorg. Chem.* **1986**, *25*, 1404.
(16) Clément, R.; Doeuff, M.; Gledel, C. *J. Chim. Phys.* **1988**, *85*, 1053.
(17) Clément, R.; et al. In *Inorganic and Organometallic Polymers with Specials Properties, NATO ASI;* Laine, R. M., Ed.; Kluwer Academic Publishers: Dordrecht, 1992; Vol. 206, p 115.
(18) Piacentini, V.; Grasso, S.; Santangelo, M. *Solid State Ionics* **1986**, *20*, 9.
(19) Boerio-Goates, J.; Lifshitz, E.; Francis, A. H. *Inorg. Chem.* **1981**, *20*, 3019.
(20) Whangbo, M. H.; Brec, R.; Ouvrard, G.; Rouxel, J. *Inorg. Chem.* **1985**, *24*, 2459.
(21) Mercier, H.; Mathey, Y.; Canadell, E. *Inorg. Chem.* **1987**, *26*, 963.
(22) Clément, R.; Girerd, J. J.; Morgenstern, I. *Inorg. Chem.* **1980**, *19*, 2852.
(23) Clément, R.; Audière, J. P.; Renard, J. P. *Rev. Chim. Miner.* **1982**, *19*, 560.
(24) Clément, R.; Lomas, L.; Audière, J. P. *Chem. Mater.* **1990**, *2*, 641.
(25) Clément, R.; Lagadic, I.; Léaustic, A.; Audière, J. P.; Lomas, L. In *Chemical Physics of Intercalation II, NATO ASI*; Bernier, P., et al., Ed.; Plenum Press: New York, 1993; Vol. 305, p 315.
(26) Lacroix, P. G.; Clément, R.; Nakatani, K.; Zyss, J.; Ledoux, I. *Science* **1994**, *263*, 658.
(27) Antonio, M. R.; Averill, B. A. *J. Chem. Soc., Chem. Commun.* **1981**, 382.
(28) Van Damme, H.; Obrecht, F.; Letellier, M. *Nouv. J. Chim.* **1984**, *8* , 681.
(29) Kauzlarich, S. M.; Teo, B. K.; Averill, B. A. *Inorg. Chem.* **1986**, *25*, 1209.
(30) Kauzlarich, S. M.; Stanton, J. L.; Fabre, J.; Averill, B. A. *J. Am. Chem. Soc.* **1986**, *108*, 7946.
(31) Bringley, J. F.; Averill, B. A.; Fabre, J. M. *Mol. Cryst. Liq. Cryst.* **1988**, *170*, 215.
(32) Kauzlarich, S. M.; Ellena, J. F.; Stupik, P. D.; Reiff, W. M.; Averill, B. A. *J. Am. Chem. Soc.* **1987**, *109*, 4561.
(33) Bringley, J. F.; Fabre, J. M.; Averill, B. A. *J. Am. Chem. Soc.* **1990**, *112*, 4577.
(34) Bringley, J. F.; Fabre, J. M.; Averill, B. A. *Chem. Mater.* **1992**, *4*, 522.
(35) Lacroix, P.; Audière, JP.; Clément, R. *J. Chem. Soc., Chem. Commun.* **1989**, 537.
(36) Lomas, L.; Lacroix, P.; Audière, JP.; Clément, R. *J. Mater. Chem.* **1991**, *1*, 475.
(37) Miyazaki, T.; Matsuzaki, S.; Ichimura, K.; Sano, M. *Solid State Commun.* **1993**, *85*, 949.
(38) Michalowicz, A. Thesis, 1990, University Paris XIII Val de Marne, France.
(39) Teo, B. K. *Inorganic chemistry concepts*; Springer-Verlag: Berlin, 1986; Vol. 9.
(40) Sayers, D. E.; Stern, E. A.; Lytle, F. W. *Phys. Rev. Lett.* **1971**, *27*, 1204.
(41) Natoli, C. R.; Benfato, M. *J. Phys.* **1986**, *47*, 12.
(42) Michalowicz, A. EXAFS pour le MAC, *Logiciels pour la chimie*, SFC: Paris, 1991; p 102.
(43) McKale, A. G. *J. Am. Chem. Soc.* **1988**, *110*, 3763.

oped at the University of Michigan.[44,45] Isomer shifts are quoted relative to iron metal at room temperature. The data are reduced and fit in Fourier space using iterative minimization procedures.[45] These procedures require that the integrated Mössbauer absorption be temperature independent. Therefore the absorber Debye–Waller factor has been modeled.[44]

Raman spectral measurements were obtained using a Raman microprobe system consisting of an inverted research microscope (Olympus, IMT-2) for illumination and scattered light collection through an Olumpus 20X/0.7NA objective. A 532 nm frequency-doubled continuous-wave Nd:YAG laser with approximately 40 mW of power was used for excitation. A ND = 2 filter was used to cut the power down to avoid sample damage. An 0.085 m axial transmissive spectrograph[46] fitted with a single-track volume phase holographic transmissive grating with a resolution of 5 cm^{-1} was used. A 532 nm holographic super notch filter was used for Rayleigh line rejection, and a thermal electrically cooled CCD camera was used for detection. Spectra were acquired using CCD9000 software (Photometrics, Ltd). Each spectrum is the result of adding together two 1 min integrations that have the dark current subtracted.

Synthesis of the $MnPS_3$–TTF Intercalate. The procedure described in ref 36 was based upon exchanging the K^+ ions of a $Mn_{1-x}PS_3K_{2x}$ preintercalate with the tetrafluoroborate salt $(TTF)_3(BF_4)_2$ in acetonitrile medium. The compound obtained under these conditions was formulated as $Mn_{0.83}PS_3(TTF)_{0.42}K_{0.10}(solv)_y$.[35] Careful reexamination of this work and more detailed analyses (particularly for the presence of remaining terafluoroborate) led to the conclusion that the potassium ions displayed in the above formula were not co-intercalated but actually present as traces of insoluble potassium tetrafluoroborate KBF_4. To clarify this issue, we designed two slightly different procedures for the synthesis:

(i) Synthesis of a tetramethylammonium intercalate $Mn_{1-x}PS_3(Me_4N)_{2x}(H_2O)_y$ and subsequent treatment of this intermediate (200 mg) with $TTF_3(BF_4)_2$ (250 mg) in acetonitrile for 2 days at 40 °C.[47] The synthesis was carried out under inert atmosphere, but the black powder eventually obtained was handled in air, where it seems stable over long periods.

Complete ion exchange was ascertained by elemental analyses, X-ray powder diffraction, and IR spectroscopy. The material obtained is well crystallized, as it exhibits sharp *hkl* reflections that can be readily indexed in a monoclinic unit cell (Table 1) closely related to that of pristine $MnPS_3$. Parameters *a* and *b* along the plane of the layers remain essentially unchanged. The interlamellar distance increases by ~5.70 Å as a result of intercalation, which strongly suggests that the TTF species stand "edge on" with respect to the $MnPS_3$ slabs, with the C=C binary axis parallel to the layers, as in the FeOCl intercalates.[29,30] We note that if an insufficient amount of $(TTF)_3(BF_4)_2$ is used, the solid collected contains a diphasic mixture of the starting tetramethylammonium intercalate and of the TTF intercalate.

Elemental analyses of the intercalate were obtained (wt %: Mn 18.0; P 12.15; S 55.3; C 12.2; H 0.7). These data led to a formula $Mn_{0.82}PS_3(TTF)_{0.42}$ close to the $Mn_{1-x}PS_3(TTF)_{\sim 2x}$ scheme. Although the electrical charges do not balance perfectly under the hypothesis of TTF^+ guest cations, the analytical data do not prove the occurrence of neutral TTF species, if one takes the experimental uncertainty in account. The overall TTF content is consistent with a value 0.40 estimated on the basis of close-packed TTF species perpendicular to the layers.

Infrared spectra of the intercalate showed evidence for the presence of TTF species (sharp bands at 1480, 830, 740 cm^{-1}, broad strong band around 1300 cm^{-1}; Figure 2). The $\nu(PS_3)$ asymmetric stretching band, which occurs at 570 cm^{-1} in pure $MnPS_3$, is split into three components at 550, 570, and 602 cm^{-1}. This band is usually split into only two components (550 and 602 cm^{-1}) in the MPS_3 intercalates, the splitting reflecting the presence of intralamellar metal vacancies.[48,49] We note that the extra component at 570 cm^{-1} appears at the same frequency as in pure $MnPS_3$. A broad continuous absorption is observed at 4000–2000 cm^{-1}, which may be related to an enhanced electronic conductivity (see below). We emphasize that a weak broad band which was observed around 1100 cm^{-1} on the previously obtained material[35] (which was thought to be a shoulder on the strong absorption band of TTF) is no longer present. This band was therefore clearly due to the BF_4^- anions present in the KBF_4 impurity.

(ii) To compare to a material obtained by a different synthetic procedure, we first treated a $Mn_{1-x}PS_3K_{2x}$ potassium intercalate with an aqueous solution of $MnCl_2$ to remove the guest K^+ ions and replace them by hexaaqua $Mn(H_2O)_6^{2+}$ species.[50] This process causes the basal spacing to rise to about 16 Å. The green powder obtained was rinsed with water and then methanol, filtered on a sintered glass and dried in air for a few minutes (without pumping under vacuum, to prevent the Mn^{2+} ions from going back into the intralayer voids). The

Table 1. Indexation of $Mn_{0.82}PS_3(TTF)_{0.42}$ at Room Temperature[a]

spacing, Å			
obsd	calcd	*hkl*	intensity
12.20	12.22	001	w
6.112	6.114	002	s
3.515	3.520	030	m
3.386	3.383	031	m
3.057	3.057	004	w
3.003	3.004	130	s
2.879	2.883	200	m
2.811	2.811	131	s
2.534	2.534	132	s
2.303	2.297	23–1	w
2.229	2.230	230	w
2.009	2.104	231	w
1.761	1.760	060	s
1.741	1.742	061	s
1.493	1.489	40–1	m
1.442	1.442	400	m

[a] Cell dimensions: $a = 6.089$ Å; $c = 12.910$ Å; $b = 10.560$ Å; $\beta = 108.70°$.

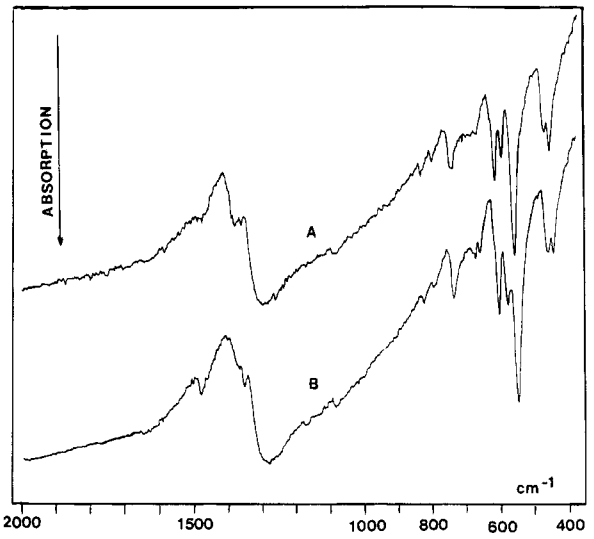

Figure 2. Infrared spectra of $Mn_{0.82}PS_3(TTF)_{0.42}$ (trace a) and of $Fe_{0.82}PS_3(TTF)_{0.38}$ (trace b).

(44) Dunham, W. R.; Wu, C. T.; Polichar, R. M.; Sands, R. H.; Harding, L. J. *Nucl. Instrum. Methods* **1977**, *145*, 537.
(45) Dunham, W. R.; Harding, L. J.; Sands, R. H. *Eur. J. Biochem.* **1993**, *214*, 1.
(46) Battey, D. E.; Slater, J. B.; Wludyka, R.; Owen, H.; Pallister, D. M.; Morris, M.D. *Appl. Spectrosc.* **1993**, *47*, 1913.
(47) Wudl, F. *J. Am. Chem. Soc.* **1975**, *97*, 1962.
(48) Mathey, Y.; Clément, R.; .Sourisseau, C.; Lucazeau, G. *Inorg. Chem.* **1982**, *6*, 2773.
(49) Sourisseau, C.; Forgerit, J. P.; Mathey, Y. *J. Solid State Chem.* **1983**, *49*, 134.
(50) Clément, R.; Michalowicz, A. *Rev. Chim. Miner.* **1984**, *21*, 426.

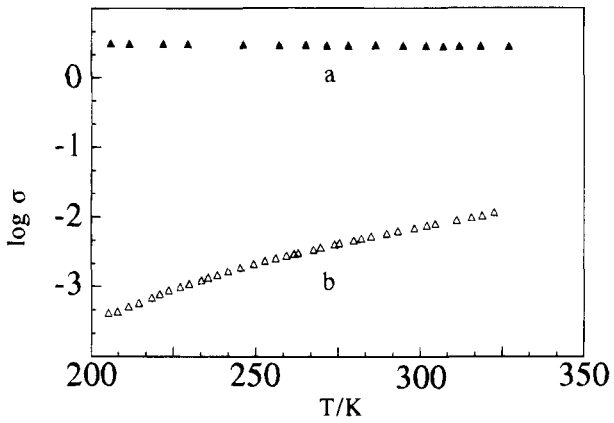

Figure 3. Temperature dependence of the conductivity σ of $Fe_{0.82}PS_3(TTF)_{0.38}$ (trace a) and of $Mn_{0.82}PS_3(TTF)_{0.42}$ (trace b) as $\log \sigma = f(T)$.

powder was then treated with a solution of $(TTF)_3(BF_4)_2$ in acetonitrile (about 12 h at 40 °C) and the material collected was characterized as above. Elemental analyses of this intercalate (wt %: Mn 19.07; P 12.6; S 56.1; C 10.65; H 0.45) led to the formula $Mn_{0.86}PS_3(TTF)_{0.36}$, again quite close to $Mn_{1-x}PS_3(TTF)_{\sim 2x}$, within experimental uncertainty. The lower TTF content and the higher Mn content (with respect to the above procedure) are probably due to fact that some Mn^{2+} ions reoccupy intralamellar sites during the treatment by $MnCl_2$.[50] The X- ray and infrared data found for this intercalate are identical to those described above.

Synthesis of the $FePS_3$–TTF Intercalate. The synthesis of this intercalate has been described by us already.[36] There are fewer degrees of freedom to perform ion exchange on $FePS_3$, as the potassium or tetramethylammonium intercalates have never been described. Attempts to obtain them have led to dissolution of the $FePS_3$ solid. Samples of the $Fe_{1-x}PS_3(TTF)_{2x}$ ($x = 0.18$) intercalate designed for Mössbauer, EXAFS, Raman, and magnetic measurements were prepared as described in our previous paper, treating a tetraethylammonium intercalate $Fe_{1-x}PS_3(Et_4N)_{2x}(solv)_y$ (400 mg) with a solution of ~500 mg of $(TTF)_3(BF_4)_2$ in dry acetonitrile (~50 mL) for 3 days at 50 °C. The starting crude $FePS_3$ powder was ground at liquid nitrogen temperature and sieved below 50 μm to minimize texture effects in the Mössbauer spectra. We confirm the analytical and structural data already published (formula $Fe_{0.82}PS_3(TTF)_{0.38}$), which are very similar to those described above for the manganese analog. The TTF species appear to stack "edge on" with respect to the $FePS_3$ slabs, with the C=C binary axis parallel to the layers. The infrared spectrum of $Fe_{0.82}PS_3(TTF)_{0.38}$ (Figure 2) also shows a broad continuous absorption (medium intensity) in the 4000–2000 cm^{-1} region, bands characteristic of the TTF species as well as splitting of the ν(PS3) band into three components (at 550, 570, and 602 cm^{-1}).

Results

Electrical Conductivity Measurements. The temperature dependence of the conductivity of $Mn_{0.82}PS_3(TTF)_{0.42}$ has been studied over the range 110–370 K, and it is represented in Figure 3. The conductivity of the intercalate ($\sigma \approx 10^{-2}$ Ω^{-1} cm^{-1} at 300 K) is considerably higher than that of pure $MnPS_3$ ($\sigma \approx 10^{-9}$ Ω^{-1} cm^{-1} at 300 K) or of pyridine intercalates.[8,51] However, the conductivity remains thermally activated with an activation energy close to 0.17 eV, estimated from the slope of the linear $\log \sigma = f(1/T)$ plot.

The dc electrical conductivity of $Fe_{0.82}PS_3(TTF)_{0.38}$ has been previously published by the authors.[36] The results are recalled in Figure 3 for the sake of clarity. The conductivity is much larger than in any other

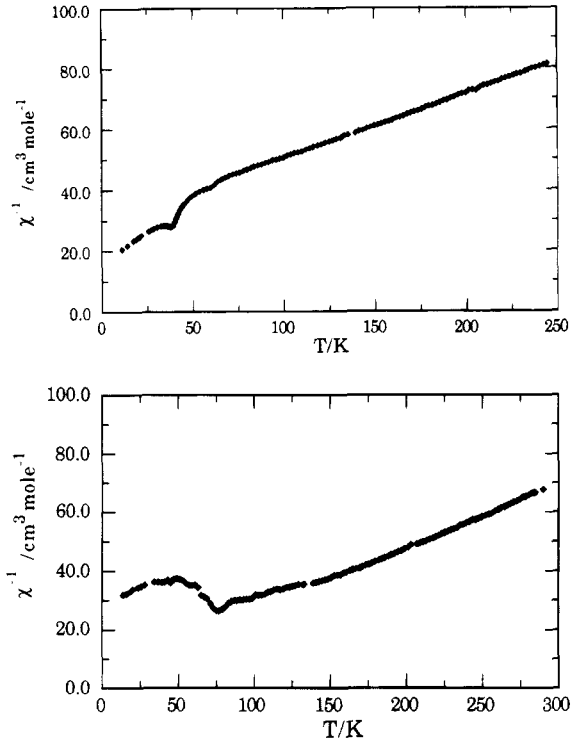

Figure 4. (a, top) Temperature dependence of the reciprocal magnetic susceptibility of $Mn_{0.82}PS_3(TTF)_{0.42}$. (b, bottom) Temperature dependence of the reciprocal magnetic susceptibility of $Fe_{0.82}PS_3(TTF)_{0.38}$.

MPS_3 intercalate ($\sigma \approx 3$ Ω^{-1} cm^{-1} at 25 °C) and, more importantly, is not thermally activated. Indeed, σ slightly increases as the temperature is lowered, a behavior which indicates a metallic character. This metallic behavior sharply contrasts with the semiconducting character of pure $FePS_3$ ($\sigma \approx 10^{-5}$ Ω^{-1} cm^{-1} at 300 K)[51] We have also measured the conductivity of the intermediate $Fe_{0.82}PS_3(Et_4N)_{0.38}$ intercalate used in the synthesis. A value of the conductivity $\sigma \approx 10^{-6}$ Ω^{-1} cm^{-1} at 300 K has been found.

Magnetic Susceptibility Measurements. The magnetic properties of the two TTF intercalates are worth studying for at least two reasons: first, to determine (particularly in the case of the metallic intercalate) whether the magnetic moments are localized or not. Second, intercalation has proved to induce ferrimagnetic properties in certain cases.[21–25]

Results are shown in Figure 4a,b, respectively: above ≈80 K, $Mn_{0.82}PS_3(TTF)_{0.42}$ shows paramagnetic Curie–Weiss behavior. The slope of the straight line above 100 K is found equal to 0.211 cm^{-3} mol K^{-1}, very close to the value expected for Mn^{2+} ions $(8/[g^2S(S+1)] = 0.228$ if $g = 2)$. This value is consistent with localized $^5/_2$ spins coupled antiferromagnetically. The antiferromagnetic interaction is much weaker than in pristine $MnPS_3$, as no susceptibility maximum can be seen. Upon cooling, χ increases rapidly between 50 and 40 K and then remains nearly constant down to 30 K. This behavior indicates the occurrence of an antiferromagnetic spin ordering (this contrasts with most $MnPS_3$ intercalates synthesized by ion exchange which become ferrimagnetic[17,25]). The continuous increase of χ at lower tem-

(51) Ichimura, K.; Miyazaki, T.; Matsuzaki, S.; Sano, M. *Mater. Sci. Forum.* **1992**, *91–93*, 505.

Table 2. Structural Parameters Extracted from the EXAFS Spectra at the Fe K-Edge of $FePS_3$ and of the $Fe_{0.85}PS_3(Et_4N)_{0.3}$ and $Fe_{0.82}PS_3(TTF)_{0.38}$ Intercalates

neighbor atom	pure $FePS_3$		$Fe_{0.85}PS_3(Et_4N)_{0.3}$		$Fe_{0.82}PS_3(TTF)_{0.38}$	
	r (Å)	σ(Å)	r (Å)	σ(Å)	r (Å)	σ(Å)
S	2.54 ± 0.01	0.12 ± 0.01	2.52 ± 0.01	0.13 ± 0.01	2.55 ± 0.01	0.12 ± 0.01
Fe	3.43 ± 0.01	0.12 ± 0.01	3.50 ± 0.01	0.14 ± 0.01	3.54 ± 0.01	0.13 ± 0.01
P	3.63 ± 0.01	0.12 ± 0.01	3.64 ± 0.01	0.17 ± 0.01	3.61 ± 0.01	0.14 ± 0.01

peratures (below 25 K) is attributed to uncoupled spins at defect sites.

The temperature dependence of the reciprocal magnetic susceptibility of $Fe_{0.82}PS_3(TTF)_{0.38}$ is shown in Figure 4b. A similar behavior is observed, and it is clear that the spins of the iron ions are localized, giving rise to temperature-dependent paramagnetism. It is more difficult to draw any quantitative information from the slope of $1/\chi$ versus temperature, as a perfectly linear behavior is not completely reached, even in the high temperature part of the curve. The slope in the range 260–290 K is equal to 0.255 cm^{-3} mol K^{-1}, which is consistent with localized iron ions in a mixed-valent state ($8/[g^2S(S+1)] = 0.285$/mol of Fe^{2+} if g is taken as 2.15 and $8/[g^2S(S+1)] = 0.228$ for Fe^{3+} ions with g = 2). Below about 75 K, the intercalate orders antiferromagnetically, but again on cooling there is an abnormal increase of χ before it drops. This point will be dicussed below.

EXAFS Characterizations. The experimental EXAFS spectrum of the $Fe_{0.82}PS_3(TTF)_{0.38}$ and its Fourier transform are shown in Figure 5a,b. The radial distribution exhibits two mains peaks. The first one (peak A) corresponds to the Fe–S distances and the second one (peak B) to unresolved Fe–P and Fe–Fe distances. With respect to pure $FePS_3$, the Fourier transform spectra of intercalates show a decrease of the intensity of the second peak. The experimental EXAFS spectra were modeled with theoretical amplitude and phases shifts calculated by McKale.[43] The pure $FePS_3$ compound was first studied, and the fits, according to X-ray diffraction data,[1,2] led us to determine the value of the electron mean free path ($\Gamma = k/\lambda = 0.81$ Å^{-2}). This Γ value, as well as the number of sulfur ($N = 6$) phosphorus ($N = 6$), and iron ($N = 3$) surrounding each iron were kept constant, considering that the overall lamellar structure is preserved and the local environment of the metal is kept octahedral. The iron–sulfur, iron–phosphorus, and iron–iron distances as well as the Debye–Waller σ parameters were allowed to vary with the absorption edge E_0. The final three shell fit (R < 2%) is presented in Figure 4c and yields the parameters shown in Table 2.

We note that in both intercalated compounds the iron–iron distances are increased compared to the value of the metal–metal distance in the pure host material. The σ parameter is the Debye–Waller factor and represents the width of the distribution of distances in a shell. Its variation for the second shell is characteristic of the local disorder around the metallic ions. We cannot fit N and σ together as they are parameters related to each other. If N decreased, σ increased, but if we try to fit the EXAFS spectra with σ constant, we find a fitting value for N that is too small according to the stoichiometry given by the chemical analysis.

The experimental EXAFS spectra recorded between 6450 and 7450 Å^{-1} (Mn K edge = 6539 eV) of $Mn_{0.82}PS_3$ $(TTF)_{0.42}$ is shown in Figure 6a and the Fourier transform (FT) is shown in Figure 6b. The fit of the EXAFS spectrum was done with the same procedure as for the $FePS_3$ based compounds. Parameters obtained from already published results on pure $MnPS_3$[52,53] were taken as references (Γ = 1.1 Å^{-2}). The parameters

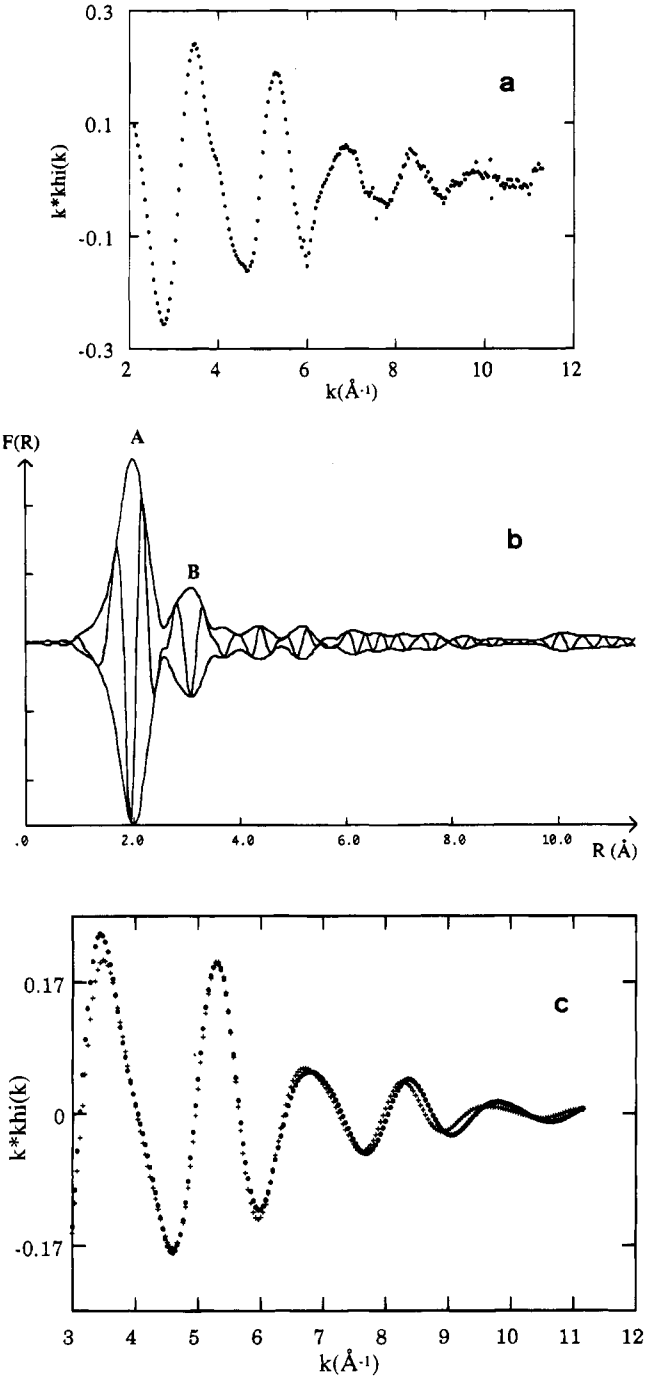

Figure 5. EXAFS data of $Mn_{0.82}PS_3(TTF)_{0.42}$. (a) Experimental absorption spectrum. (b) Fourier transform. (c) Filtered (+) and simulated (●) spectra.

(52) Michalowicz, A.; Clément, R. *Inorg. Chem.* **1982**, *21*, 3872.

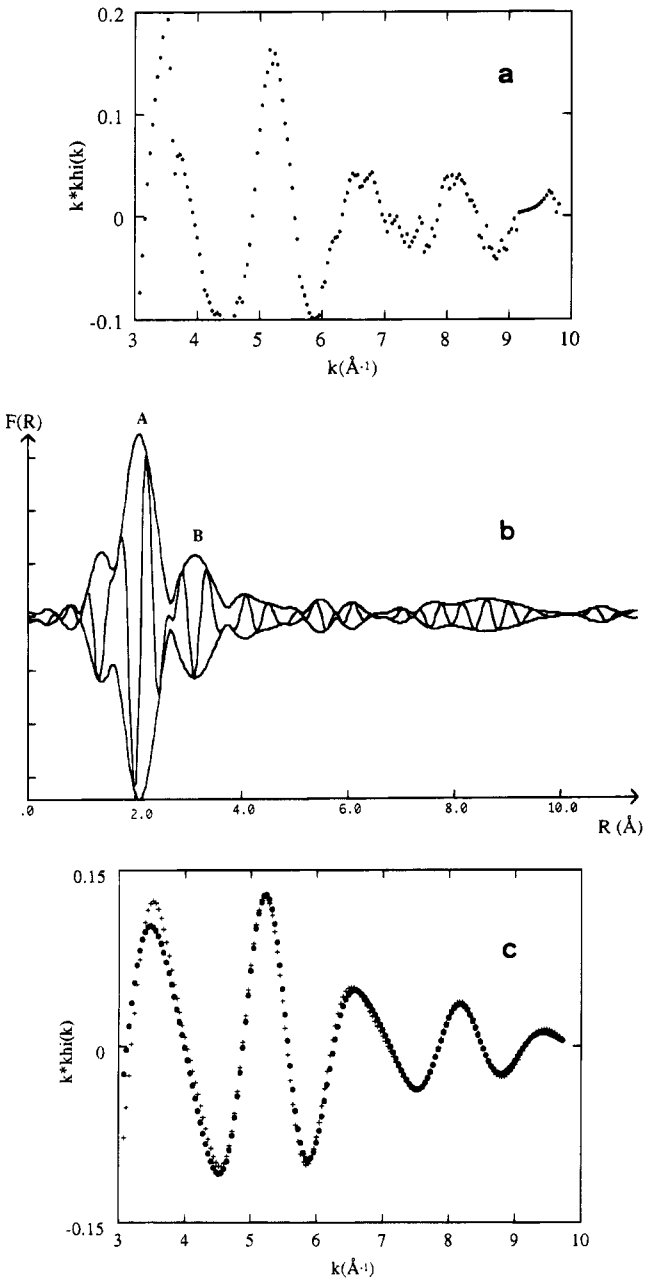

Figure 6. EXAFS data of $Fe_{0.82}PS_3(TTF)_{0.38}$. (a) Experimental absorption spectrum. (b) Fourier transform. (c) Filtered (+) and simulated (●) spectra.

extracted from the final three shells fit (R < 3.4%, Figure 5c) are shown in Table 3: The environment of the manganese atoms is not drastically modified by the insertion of the TTF cations, but again intercalation significantly increases the Mn−Mn distance, as noted above for the $FePS_3$ intercalates. Intercalation also strongly increases the width of the distance distribution in the second shell.

^{57}Fe Mössbauer Spectroscopy. In the search for possible mixed valency in the TTF intercalates, we recorded the Mössbauer spectra of pure $FePS_3$, of the $Fe_{0.82}PS_3(TTF)_{0.38}$ intercalate, as well as that of the intermediate tetraethylammonium intercalate $Fe_{0.85}PS_3(Et_4N)_{0.3}$. Powders were sieved below 50 μm to reduce anisotropic texture effects. The spectrum of $FePS_3$

(53) Gledel, C.; Audière, J. P.; Clément, R.; Cortes R. *J. Chim. Phys.* **1989**, *86*, 1691.

Table 3. Structural Parameters Extracted from the EXAFS Spectra at the Mn K-Edge of $MnPS_3$ and $Mn_{0.82}PS_3(TTF)_{0.42}$ Intercalate

neighbor atom	pure $MnPS_3$		$Mn_{0.82}PS_3(TTF)_{0.42}$	
	r (Å)	σ (Å)	r (Å)	σ (Å)
S	2.58 ± 0.02	0.08 ± 0.01	2.60 ± 0.01	0.11 ± 0.01
Mn	3.47 ± 0.02	0.09 ± 0.01	3.56 ± 0.01	0.12 ± 0.01
P	3.70 ± 0.02	0.08 ± 0.01	3.72 ± 0.01	0.17 ± 0.01

Table 4. Parameters Extracted from the ^{57}Fe Mössbauer Spectra of Pure $FePS_3$ and of the $Fe_{0.85}PS_3(Et_4N)_{0.3}$ and $Fe_{0.82}PS_3(TTF)_{0.38}$ Intercalates

composition		δ (mm s^{-1})	ΔE_q (mm s^{-1})	intensity
$FePS_3$		0.99	1.57	1.00
$Fe_{0.85}PS_3(Et_4N)_{0.3}$	A	1.01	2.50	0.46
	B	1.00	1.85	0.54
$Fe_{0.82}PS_3(TTF)_{0.38}$	A	1.01	2.56	0.28
	B	1.00	1.75	0.58
	C	0.34	0.82	0.14

(shown in Figure 7a) consists of a doublet characterized by an isomer shift of 0.99 mm/s and a quadrupole splitting of 1.57 mm s^{-1}, in agreement with previously published data,[12] although a slight inequivalence in these sites manifests itself in a larger line width of the left-hand line compared to the right-hand line. These values correspond to Fe(II) ions occupying crystallographically equivalent sites. The spectrum of the $Fe_{0.85}PS_3(Et_4N)_{0.3}$ intercalate is shown in Figure 7b. It consists of two doublets **A** and **B** having the same isomer shift but a different quadrupole splitting. The intensities of theses doublets are (46% for type A, 54% for type B, Table 4). This spectrum reveals that all iron atoms remain in the +2 oxidation state but also that there are two types of Fe(II) iron atoms located on two nonequivalent sites. We emphasize the fact that the spectrum does not show any signal that would indicate iron atoms in the +3 oxidation state.

The spectrum of the $Fe_{0.82}PS_3(TTF)_{0.38}$ intercalate is shown in Figures 7c,d. This spectrum also exhibits the two types of A and B doublets described above, actually with a different intensity ratio. However, the spectrum exhibits an additional doublet (C) with an isomer shift δ = 0.34 mm s^{-1} and a quadrupole spitting ΔEq = 0.82 mm s^{-1}. Simulation and fitting procedures show that this C peak can be readily accounted for by a model assuming the occurrence of 14% of ferric Fe^{3+} ions in the intercalate. The ferric peak becomes sharper as the temperature is increased (Figure 7d), due to the lessening of magnetic splitting brought about by spin relaxation; The ferric ions are therefore involved in spin coupling or some other magnetic interaction that leads to spatial quantization at low temperature, such as zero field splitting interaction. It is not possible from the Mössbauer spectra alone to conclude that any of the iron is spin coupled, but this is likely to be the case, in view of the magnetic properties of these materials.

Raman Spectroscopy. The Raman spectrum of a powdered sample of the $Fe_{0.82}PS_3(TTF)_{0.38}$ intercalate (Figure 8) shows peaks at 504 and 760 cm^{-1} and a group of three peaks which partially overlap in the 1400−1500 cm^{-1} region (1412, 1494, and 1520 cm^{-1}). Reference to the numerous articles published on the Raman spectroscopy of the MPS_3 phases and of the tetrathiafulvalene family unambiguously shows that theses peaks originate from TTF species.[48,54,55] The peaks in the 1400−1500 cm^{-1} region are of special interest, as they

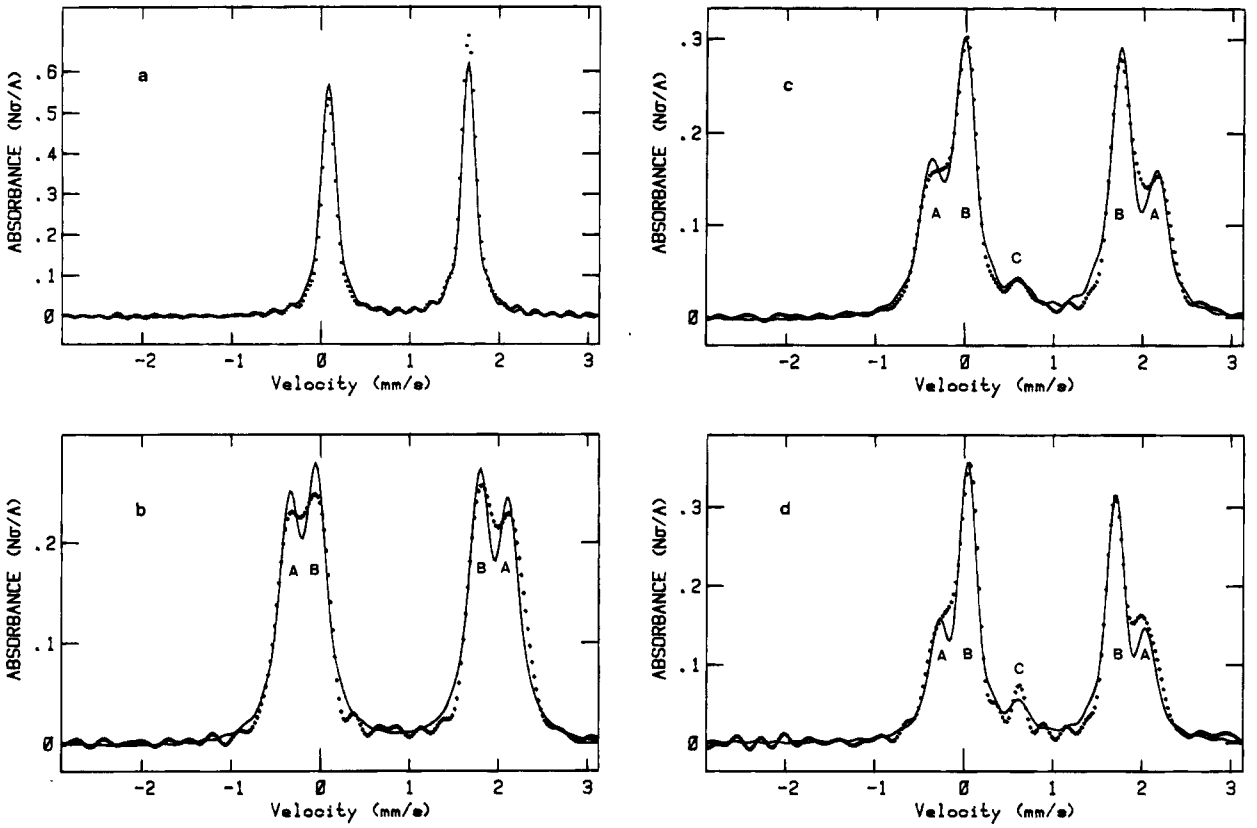

Figure 7. Mössbauer spectra of (a) $FePS_3$ at 125 K, (b) $Fe_{0.85}PS_3(Et_4N)_{0.3}$ at 125 K. (c) $Fe_{0.82}PS_3(TTF)_{0.38}$ at 125 K and (d) $Fe_{0.82}PS_3(TTF)_{0.38}$ at 300 K. In (a–c) the experimental data (dots) were fit by a simulation program according to the parameters in Table 4. In (d), the 300 K data were fit with the same intensities as with (c), but with slightly different line positions.

are very sensitive to the electronic structure of the TTF species. Actually the frequency of the a_g ν_3 mode (central C=C stretching) has been shown to shift from 1516 cm^{-1} for a neutral TTF species to 1420 cm^{-1} for a fully ionized TTF^+ species[54,55] with a linear relation between the frequency shift and the degree of ionicity. Therefore, the peaks at 1412 and 1520 cm^{-1} observed in the spectrum of the $Fe_{0.82}PS_3(TTF)_{0.38}$ intercalate reflect the presence of "localized" TTF° and TTF^+ species, whereas the peak at 1494 cm^{-1} may reflect the presence of TTF species in a delocalized mixed valent state.

Discussion

The set of results described above clearly shows that the MPS_3–TTF intercalates have magnetic and electrical properties markedly different from those of most intercalates prepared by ion exchange in the MPS_3 family. The pure $MnPS_3$ and most intercalates such as $Mn_{1-x}PS_3(Et_4N)_{2x}$ are rather insulating (conductivity about 10^{-8} Ω^{-1} cm^{-1} at 300 K), whereas $Mn_{0.86}PS_3(TTF)_{0.36}$ has a much higher conductivity (10^{-2} Ω^{-1} cm^{-1} at 300 K) and a low activation energy. The contrast is even stronger for the $FePS_3$ analogues, where $Fe_{0.82}PS_3(TTF)_{0.38}$ takes a metallic character. An important structural feature of both TTF intercalates is that the guest species lie "edge on" in the interlayer space (a result well established for the FeOCl analogues[29–32]) and also confirmed by the spectroscopic investigations of Miyazaki et al.[37] for the intercalate of TTF in $MnPS_3$. This contrasts with the behavior of planar guest species such as pyridinium, 4,4′-dipyridinium or methylviologen which we have observed to lie with their molecular plane parallel to the layers once inserted. Such "edge on" orientation is favorable to the formation of aggregates or even possibly stacks of TTF species. The TTF content is actually consistent with close packing.

The key point of our results is the indication that 14% of the iron atoms in the $Fe_{0.82}PS_3(TTF)_{0.38}$ intercalate are in the +3 oxidation state, in contrast to pure $FePS_3$ and $Fe_{1-x}PS_3(Et_4N)_{2x}$ which only contain Fe^{2+} ions. This feature may originate from partial electron transfer between the host lattice and the guest species, more precisely from the oxidation of part of the Fe^{2+} ions by TTF^+ species. Such a transfer is expected to induce mixed valency in both the host and the guest sublattices. Therefore, although this intercalate is synthesized by ion exchange (Et_4N^+/TTF^+), the internal Fe^{2+}/Fe^{3+} and $TTF^+/TTF°$ redox couples would equalize their potential and give mixed valency. This model, taken together with a stacked arrangement of the guest species, provides a possible explanation for the metallic properties of the $Fe_{0.82}PS_3(TTF)_{0.38}$ intercalate. However, the results obtained by Raman spectroscopy show that the situation is more complex, as all the TTF species are not in a unique delocalized mixed valence state. The three peaks observed in the range 1400–1500 cm^{-1} seem to indicate that the inserted species are "grouped" in three types of domains: a first type consisting of neutral TTF molecules only, a second type consisting of fully ionized TTF^+ cations, and a third type consisting of mixed valent species that could possibly account for

(54) Bozio, R.; Zanon, I.; Girlando, Pecile, C. *J. Chem. Phys.* **1979**, *71*, 2282.
(55) Matsuzaki, S.; Moriyama, T.; Toyoda, K. *Solid State Commun.* **1980**, *34*, 857.

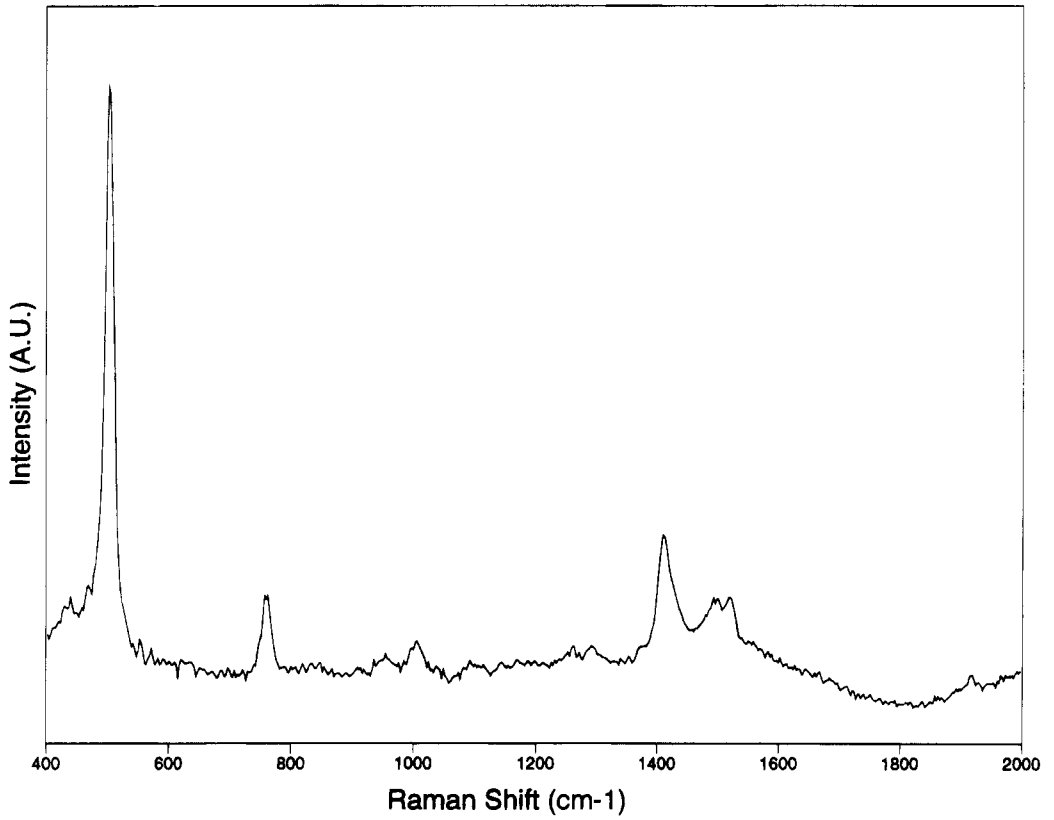

Figure 8. Raman spectrum of the $Fe_{0.82}PS_3(TTF)_{0.38}$ intercalate.

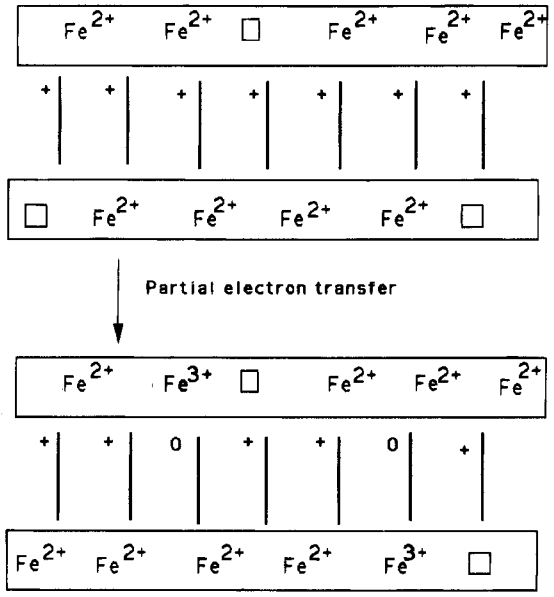

Figure 9. Model of the host-to-guest electron transfer invoked to explain the metallic character of $Fe_{0.82}PS_3(TTF)_{0.38}$.

the high metallic-type conductivity (Figure 9). It can be noted that the occurrence of 14% of ferric ions in the $Fe_{0.82}PS_3(TTF)_{0.38}$ formulation would imply that only 0.12 TTF^+ are reduced to the zero oxidation state by the electron transfer, which leaves a substantial amount of nonreduced TTF^+ species, in agreement with the predominant intensity of the Raman peak at 1412 cm^{-1}. The presence of domains consisting of neutral TTF species could also account for the more complex splitting of the $\nu(PS_3)$ mode in the infrared spectrum of $Fe_{0.82}PS_3(TTF)_{0.38}$. The additional band which appears at 570 cm^{-1} (same wavenumber as in pure $FePS_3$) may indicate that domains with local composition MPS_3 (having no intralayer vacancies) are being reconstructed upon the synthesis from the $Fe_{1-x}PS_3(Et_4N)_{2x}$ preintercalate and therefore the occurrence of neutral TTF species in such neutral domains would not violate electroneutrality.

Manganese(II) ions are more difficult to oxidize than Fe(II) ions, and the fact that the $Mn_{0.82}PS_3(TTF)_{0.42}$ intercalate remains semiconducting may be a consequence of this difference. Nevertheless, this material has a conductivity much higher than usual $MnPS_3$ intercalates by a factor of about 10^5 (as noted above). Miyazaki et al. have recently shown[37] that the TTF species in $Mn_{0.82}PS_3(TTF)_{0.42}$ were in a state of mixed valence, on the basis of electronic and Raman spectra. They also came to the conclusion that the intermolecular interactions between TTF species confined in $MnPS_3$ were stronger than in TTF radical salts. The relatively high conductivity found for this material supports this conclusion. Also our analytical data indicate a slight excess of positive charge with respect to the manganese deficit if all the TTF species were counted as being cationic; this is also in agreement with mixed valency in the TTF sublattice.

The small but significant increase of the M−M bond length (observed by EXAFS) accompanying intercalation of Et_4N^+ and TTF^+ into both $MnPS_3$ and $FePS_3$ reveals slight structural modifications of the host lattice accompanying intercalation. A number of facts are now known that indicate or imply that the symmetry of the MPS_3 host lattice is considerably lowered once intercalated: Infrared and Raman studies have shown that the center of symmetry in pristine $MnPS_3$ is removed upon intercalating pyridine.[56] Luminescence spectra of

(56) Joy, P. A.; Vasudevan, S. *J. Am. Chem. Soc.* **1992**, *114*, 7792.

intercalated rare-earth cations show strong Stark effects due to a very low local symmetry[57] of the environment. The recent finding of strong quadratic nonlinear optical properties of MPS_3–stilbazolium intercalates[26] implies that the latter has a noncentrosymmetrical space group. Atomic force microscopy studies of the surface of MPS_3 crystals carried out in our group have shown that the position of the sulfur atoms are strongly modified after intercalation because of the tilting of the PS_3 pyramids of the host lattice.[58] The Mössbauer spectra of the tetraethylammonium and TTF intercalates described in this paper show that the Fe^{2+} ions are located on different sites after intercalation. This feature also is consistent with a symmetry lowering accompanying intercalation. Such a redistribution of the Fe^{2+} ions over different sites may also explain variations in the average M–M distances after and before intercalation.

Several other features are worth addressing: in the first place, we emphasize that both TTF intercalates order antiferromagnetically at low temperature, whereas many MPS_3 intercalates take up a net magnetization due to spin balance destruction caused by the metallic vacancies.[25,59] As noted above, the magnetic susceptibility slightly increases as the temperature goes down just prior to antiferromagnetic ordering. It can be suggested that although there may be spin noncompensation occurring within individual slabs, the resulting magnetic moments on adjacent slabs eventually order in an antiparallel way as the temperature goes down through T_c. The antiferromagnetic interlayer coupling necessary to account for this feature may be the consequence of quite strong interactions between the sulfur atoms of the $FePS_3$ slabs and the sulfur atoms of the inserted TTF^+ radicals.

(57) Clément, R.; Léaustic, A.; Marney, K.; Francis, A. H. *J. Phys. Chem. Solids* **1994**, *55*, 9.
(58) Lagadic, I.; Clément, R.; Kahn, O.; Ren, J.; Whangbo, M. *Chem. Mater.* **1994**, *6*, 1940.
(59) Evans, J. Thesis, 1994, University of Oxford, U.K.

Conclusion

Insertion of TTF^+ cations into the MPS_3 host lattices can be achieved under quite mild conditions and allows the synthesis of a new type of organic–inorganic metal. Although some features cannot be fully described yet, we think that these results confirm that the area of intercalation can bring new opportunities in the area of molecular metals. The host lattice might favor the appearance of superconductivity at low temperature if it is able to hinder the Peierls transitions. The vast possibility of metal substitution in the MPS_3 family should allow one to modify and control the degree of mixed valency of the guest species. Also, there is a large variety of such organic cations with different redox potential that can be brought in intimate contact with inorganic slabs and hence a wealth of low-dimensional, well crystallized new composites are to be explored.

Acknowledgment. The authors thank the staff of L.U.R.E. (Orsay) for operating the DCI storage ring. International collaboration was greatly assisted by funds from the NATO research program. The authors are greatly indebted to W. Kowalchyk and M. D. Morris (University of Michigan) who have carried out the Raman analyses.

CM940354N